Int J Adv Manuf Technol (2013) 66:363–370
DOI 10.1007/s00170-012-4330-x

ORIGINAL ARTICLE

Analysis of heat transfer coefficient on workpiece surface during minimum quantity lubricant grinding

Cong Mao · Hongfu Zou · Yong Huang · Yafei Li · Zhixiong Zhou

Received: 18 December 2011 / Accepted: 21 June 2012 / Published online: 4 July 2012

Abstract The surface heat transfer exhibits highly nonlinear characteristic during minimum quantity lubrication (MQL) grinding owing to the high grinding surface temperature gradient, the complicated movement characteristic of the spray and the random droplet size. Based on the atomization mechanism, the influencing factors about the velocity and the diameter of the droplet were analyzed. The grinding zone was divided into four different regions according to the heat transfer mechanism of the droplet at different surface temperatures, namely non-boiling heat transfer region, nucleate boiling heat transfer region, transitional boiling heat transfer region and stable film boiling heat transfer region. Furthermore, the related mathematical models of heat transfer in the grinding zone were established. The surface grinding experiment is carried out; a good agreement is found between the simulative result and experimental measuring result of the surface temperature during MQL grinding, which shows that the theory of surface heat transfer coefficient during MQL grinding is creditable.

Keywords Heat transfer coefficient · MQL grinding · Boiling · Spray

1 Introduction

The grinding energy ratio is very high during the grinding process, especially for hard-to-cut materials. Moreover, most of the grinding energy is converted into grinding heat and accumulated in the grinding zone. If this grinding heat cannot be taken away in time, the temperature in grinding zone would be risen sharply, which has serious influence on the quality and service life of the component [1]. Therefore, looking for an effective cooling method has great significance on controlling the grinding temperature and improving the workpiece quality. Cooling techniques usually include traditional wet cooling, steam cooling, liquid nitrogen cooling, cold air cooling, jet impinging wet cooling and minimum quantity lubrication (MQL) technique. From the cooling effect, economic, environmental protection and so on, the MQL technique is regarded as a kind of more effective green cooling technology [2]. Although MQL technique is widely applied in drilling [3], milling [4] and turning [5], MQL grinding is still a relatively new research area. Previous research [6] found that an enhanced grinding performance was obtained with lower grinding force, decreased wheel wear, improved surface roughness and residual compressive stresses in comparison with dry grinding.

It is obvious that the spraying process is dynamic and is affected by various factors. In addition, the contact heat transfer depends strongly on the impacting droplet dynamics, and in turn, the droplet dynamics depend on the diameter and impinging velocity of the droplet. Meanwhile, the heat transfer during MQL grinding is a complex nonlinear system. When grinding temperature is risen up to a certain extent, the droplets entering into grinding zone would momentarily be boiled and vaporized [7, 8]. Therefore, the research of heat transfer coefficient during MQL grinding is more difficult.

Based on the atomization mechanism, the effect of the pressure of air and liquid, air–liquid ratio, liquid properties and nozzle parameters on the diameter and the impinging velocity of the droplet were investigated in this study. According to the heat transfer mechanism of the droplet under different surface temperatures, the grinding zone

C. Mao (✉) · H. Zou · Y. Huang · Y. Li
College of Automotive and Mechanical Engineering,
Changsha University of Science and Technology,
Changsha 410114, China
e-mail: maocong315@yahoo.com.cn

Z. Zhou
College of Mechanical and Vehicle Engineering,
Hunan University,
Changsha 410082, China

was divided into four different regions, namely non-boiling heat transfer region, nucleate boiling heat transfer region, transitional boiling heat transfer region and stable film boiling heat transfer region. In addition, the related mathematical models of heat transfer in the grinding zone were established. Furthermore, the surface grinding experiment was carried out to validate the theory of surface heat transfer coefficient during MQL grinding.

2 Spraying parameters

The MQL technique has a better heat transfer effect on grinding zone because the droplets can break through the barrier layer of gas around the grinding zone and be injected into the grinding zone [9, 10]. But it cannot be achieved in the traditional wet grinding. Thus, the heat transfer effect of MQL technique depends on the droplet impinging force. It is known that the droplet impinging force depends strongly on the momentum of the impacting droplet, and in turn, the droplet momentum depends on the diameter and the impinging velocity of the droplet. Therefore, the diameter and the impinging velocity of the droplet have a significant effect on the heat transfer effect on grinding zone.

The MQL system is shown in Fig. 1. In this system, the compressed air which is supplied by the air compressor enters into the gas inlet pipe. Moisture and dust are excluded by the air filter, and a small quantity of compressed air is used to control pneumatic pump by the frequency generator. The grinding fluid is conveyed to the liquid inlet pipe. The compressed air passes through the flow rate adjustment and then is mixed with grinding liquid in the nozzle. The workpiece and grinding wheel is cooled and lubricated when the atomized grinding fluid is injected into the grinding zone with a high velocity. In addition, the flow rate of grinding fluid is controlled by a flow rate adjustment.

The internal-mixing two-phase flow nozzle is employed in the MQL equipment. The grinding liquid tube with a smaller diameter is installed in the air tube with a larger diameter, and the axes of the two tubes coincide with each other. The compressed air is transported by the air tube, and the grinding liquid is injected into the liquid tube. The compressed air and the grinding fluid are mixed in the nozzle. It is obvious that the velocity of the air is very high, but the velocity of the liquid is quite slow, and then the relative velocity between the liquid and the air is very high. Therefore, there is a greater frictional force between the air and the liquid, and thus the grinding liquid can be split into droplets with a micron grade diameter.

According to the Bernoulli equation [11], the relation of the droplet velocity at the nozzle exit v_0, the cooling liquid flow rate Q_l and the pressure of the compressed air p_a can be expressed by:

$$v_0 = \sqrt{\frac{\frac{P_a - P_0}{\rho_l} + \frac{16Q_l^2}{\pi^2 D^2}}{1+\xi}} \tag{1}$$

where p_0 is the atmosphere pressure, ρ_l is the cooling liquid density, D is the nozzle diameter, and ξ is the resistance coefficient.

It is known that the gravity force of the droplet is quite small in comparison with the resistance of the ambient air before the droplet is collided with the contact zone between the grinding wheel and the workpiece. Thus, only the effect of the resistance of ambient air on the velocity of the droplet is considered. The velocity of the ambient air is very low in comparison to that of the droplet, and then the ambient air can be considered as static. Thus, the velocity of the droplet v_l before it is collided with the grinding zone can be expressed as [11]:

$$v_l = \frac{2v_0}{1+\sqrt{\frac{2C_D S_e \gamma_a v_0 t}{mg}+1}} \tag{2}$$

where C_D is the air resistance coefficient, S_e is the section area of the droplet, and γ_a is the gravity of air.

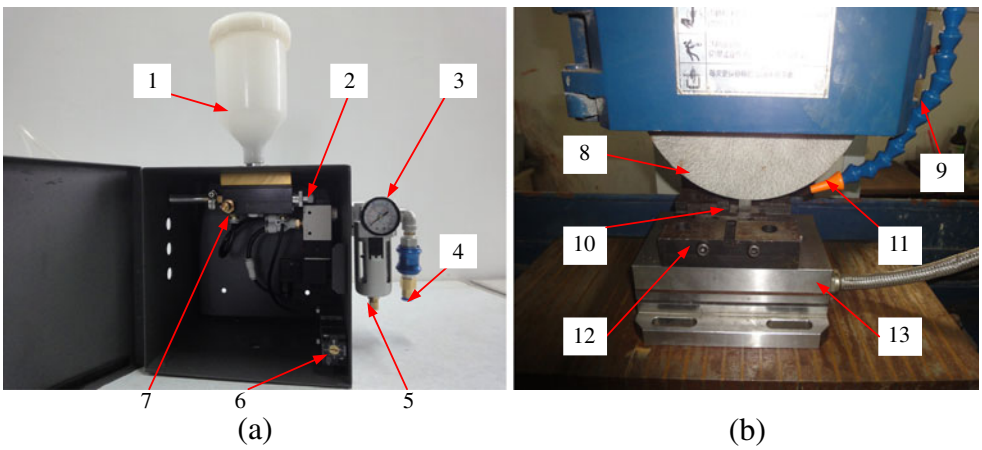

Fig. 1 **a** The MQL system: *1* reservoir, *2* grinding fluid flow rate adjustment, *3* manometer, *4* air inlet, *5* air filter, *6* frequency generator, *7* pneumatic pump for individual adjustment. **b** The MQL grinding experimental equipment: *8* grinding wheel, *9* double layers tube, *10* workpiece and thermocouple, *11* nozzle, *12* clamping device, *13* dynamometer

It is known that the distance between the nozzle and the grinding zone is very small (about 25–40 mm in this study), and there also exists a dip angle between the nozzle and the grinding zone. Then, it only takes a relatively short time when the droplet is injected into the grinding zone from the exit of the nozzle. According to Eq. (2), the velocity of the droplet v_l before it is collided with the grinding zone is really close to the spraying velocity of the droplet at the nozzle exit v_0.

The compressed air and the liquid are mixed in the nozzle, and the liquid is split into droplet by the compressed air. According to the reference [12], the average diameter of the droplets is calculated as follows:

$$d = \frac{585\sqrt{\delta}}{v_r\sqrt{\rho_l}} + 597\left[\frac{\mu_l}{\sqrt{\rho_l\delta}}\right]^{0.45} \times \left(1000\frac{Q_l}{Q_a}\right)^{1.5} \quad (3)$$

where δ is the surface tension of the cooling liquid, ρ_l is the density of the cooling liquid, v_r is the relative velocity between the air and the liquid, μ_l is the viscosity of the cooling liquid, Q_l is the flow rate of the cooling liquid, and Q_a is the flow rate of the air.

Based on Eq. (3), the ratio of Q_l to Q_a, the viscosity of the cooling liquid μ_l, the density of the cooling liquid ρ_l and the relative velocity v_r between the air and the liquid are the important factors that influence the droplet diameter.

The different velocity of the droplets at the nozzle exit can be obtained by changing the pressure of the compressed air when the nozzle and cooling liquid were selected. In addition, as the pressure of the compressed air is increased, the flow rate of the compressed air increases. The diameter of droplets is affected by the ratio of Q_l to Q_a. Therefore, the pressure of compressed air and the flow rate of cooling fluid are the major factors that affect the velocity and diameter of droplets during spraying.

3 The surface heat transfer mechanism during MQL grinding

It is well known that there are three different heat transfer mechanisms in the MQL technique [8, 13]: (1) droplet contact heat transfer, (2) air convective heat transfer and (3) radiation heat transfer. The radiation heat transfer can be usually neglected when the surface temperature is less than 800 °C [8]. Based on the experiment of dry grinding, the authors found that the peak temperature in the grinding zone during dry grinding does not exceed 800 °C under the given grinding parameters in this study. It is obvious that the peak temperature for MQL grinding is lower than that for dry grinding. Therefore, the radiation heat transfer is neglected. The temperature distribution in grinding zone is varied along the grinding direction, and the heat transfer is closely related to surface temperature. According to the heat transfer mechanism of the droplet at different surface temperatures and the temperature distribution in the grinding zone, the heat transfer in grinding zone can be divided into four parts: non-boiling heat transfer (when the surface temperature T_W is less than 105 °C), nucleate boiling heat transfer (105 °C < T_W < 125 °C), transition boiling heat transfer (125 °C < T_W < 300 °C) and stable film boiling heat transfer (300 °C < T_W).

For simplifying the computational process, the heat transfer model of MQL grinding in the grinding zone is simplified as follows:

(1) The heat source of grinding surface is derived from the friction between the grinding wheel and the workpiece. It is assumed that a constant heat flux load is applied on the microscopic subunits of grinding surface per unit time.
(2) It is known that the velocity of droplet is higher than that of the grinding wheel. Furthermore, the nozzle is angularly positioned toward the grinding wheel. Therefore, it can be assumed that the droplet can break through the gas barrier layer around the grinding wheel surface, and then the droplet can be injected into the grinding zone.
(3) The volume flow rate of air is 5–6 orders of magnitude larger than that of the liquid. It can be assumed that the heat transfer style of the air is convection, and the heat transfer style of the droplet is only considered as boiling heat transfer.
(4) The interaction of droplets can be ignored since the density of them is quite small.
(5) The droplet can be kept to a spherical shape when it is collided with the gas layer on the grinding wheel surface.
(6) The droplet diameter is quite small so that they can be heated to the grinding surface temperature in a moment.
(7) In the high temperature zone, the temperature of vapor near the grinding surface is assumed as the same with grinding surface temperatureT_W. The temperature of vapor contact with liquid film is considered as the saturated temperature of liquid T_S.

3.1 Non-boiling heat transfer

When the grinding temperature is below 105 °C, it cannot make the droplet phase change. Therefore, this region is non-boiling heat transfer. The ratio of the flow rate of the air Q_a to the flow rate of the cooling liquid Q_l is quite large, and then the heat transfer in this region only included two parts: air convective heat transfer and droplet contact heat transfer.

The heat transfer coefficient of air convective h_a can be expressed as [14]:

$$h_a = \frac{\lambda_a \mathrm{Nu}}{l} \quad (4)$$

$$\mathrm{Nu} = 0.906\mathrm{Re}^{\frac{1}{2}}\mathrm{Pr}^{\frac{1}{3}} \tag{5}$$

$$\mathrm{Re} = \frac{v_{\mathrm{a}}^{'}\rho_{\mathrm{a}}l}{\mu_{\mathrm{a}}} \tag{6}$$

$$h_{\mathrm{a}} = 0.906\mathrm{Re}^{\frac{1}{2}}\mathrm{Pr}^{\frac{1}{3}}\frac{\lambda_{\mathrm{a}}}{l} \tag{7}$$

where λ_{a} is the thermal conductivity of air, Nu is the Nusselt number, Re is the Reynolds number, Pr is the Prandtl number, l is the width of heat transfer in grinding zone, $v_{\mathrm{a}}^{'}$ is the velocity of the air, ρ_{a} is the density of the air, and μ_{a} is the viscosity of the air.

The heat transfer coefficient of droplet contact h_{l} can be expressed as:

$$h_{\mathrm{l}} = \frac{q_{\mathrm{l}}}{T_{\mathrm{w}} - T_{\mathrm{l}}} \tag{8}$$

$$q_{\mathrm{l}} = C_{\mathrm{l}}m(T_{\mathrm{w}} - T_{\mathrm{l}}) \tag{9}$$

where C_{l} is the specific heat of the droplet, m is the quality of the droplet that participated in heat transfer, T_{w} is the grinding zone temperature, and T_{l} is the initial temperature of the droplet.

The total heat transfer coefficient can be expressed as:

$$h = h_{\mathrm{a}} + h_{\mathrm{l}} \tag{10}$$

In the non-boiling heat transfer region, there is a nearly linear relation between the grinding zone temperature and the heat transfer quantity which is carried by MQL technique [11]. The heat transfer coefficient is the ratio of the heat transfer quantity to the temperature difference between the grinding zone temperature and the initial temperature of the grinding liquid. Therefore, the heat transfer coefficient can be approximately regarded as a constant in this region.

3.2 Nucleate boiling heat transfer and transition boiling heat transfer

In this region, the droplet is formed as a very thin liquid film on the heat transfer surface when the temperature is low, and which performs as the general boiling characteristics. The liquid film will be broken with the increasing of the surface temperature, which causes local liquid film section and dry section to be coexisted on the heat transfer surface. The heat transfer reaches to the peak value when the liquid film is completely vaporized. It shows a stable transition boiling rather than a film boiling when the temperature continues to rise.

Therefore, the heat transfer quantity is quite complex in the nucleate boiling and transition boiling heat transfer region, and it performs a non-linear relation with the surface temperature. It is difficult to accurately estimate the heat transfer coefficient at different surface temperatures. Based on this problem, a large number of experimental and theoretical researches have been carried out [15–19]. But the results differ since the experimental parameters and the environment are different. However, these results show that there is a common characteristic; namely, the relation between the heat transfer quantity and the surface temperature is an analogous parabolic distribution. In the nucleate boiling region, the curve is steeper with the rising of the temperature. The heat transfer reaches to the peak value at the critical point of 125 °C and then drops down rapidly in the transition boiling region. In the transition boiling region, the curve becomes smooth with the rising of temperature. Nevertheless, the heat transfer coefficient is the ratio of heat transfer quantity to the temperature difference between the grinding surface temperature and the initial temperature of the grinding liquid. After the parabolic curve function is analyzed, it can be concluded that as the temperature increases, the heat transfer coefficient will increase in the nucleate boiling region, but it will decrease in the transition boiling region. At the point of critical heat flux, it reaches to the peak value.

The critical heat flux is as follows [15]:

$$q_{\max} = \varepsilon[h_{\mathrm{fa}} + C_{\mathrm{l}}(T_{\mathrm{S}} - T_{\mathrm{l}})]\phi + q_{\mathrm{a}}^{'} \tag{11}$$

$$q_{\mathrm{a}}^{'} = 0.906\mathrm{Re}^{\frac{1}{2}}\mathrm{Pr}^{\frac{1}{3}}\frac{\lambda}{l}(T_{\mathrm{W}} - T_0) \tag{12}$$

where ε is the ratio of the droplet that participated in evaporation, h_{fa} is the latent heat of vapor, C_{l} is the specific heat of the droplet, T_{S} is the saturation temperature of the droplet, T_{l} is the initial temperature of the droplet, ϕ is the mass flow rate of the liquid, and $q_{\mathrm{a}}^{'}$ is the heat transfer quantity of the air.

The momentum of the droplet is quite large, and then the part of the droplets which are taken away by the vapor in the grinding zone can be neglected. Hence, it is assumed that all the droplets are evaporated in the heat transfer surface (the value of ε is set to 1). Equation (11) can be simplified as:

$$q_{\max} = [h_{\mathrm{fa}} + C_{\mathrm{l}}(T_{\mathrm{S}} - T_{\mathrm{l}})]\phi + q_{\mathrm{a}}^{'} \tag{13}$$

Therefore, the heat transfer coefficient in the point of critical heat flux can be expressed as:

$$h_{\max} = \frac{q_{\max}}{T_{\mathrm{W}} - T_{\mathrm{l}}} \tag{14}$$

3.3 Stable film boiling heat transfer

The film boiling of MQL technique is slightly different from pool film boiling, but the mechanism is fairly similar. Based on the pool film boiling, the mathematical model is revised, and a revised heat transfer mathematical model of film boiling for MQL technique is obtained. The heat transfer in this region includes the droplet contact heat transfer, the air convective heat transfer and the radiation heat transfer. As mentioned in "Section 3", the radiation heat transfer can be neglected when the surface temperature is less than 800 °C. Therefore, only the droplet contact heat transfer and the air convective heat transfer are considered in this model.

The heat transfer quantity of single droplet contact with a hot surface can be expressed as [8]:

$$q_{\mathrm{d}} = \frac{\pi d^3}{6}\rho_{\mathrm{l}}[h_{\mathrm{fa}} + C_{\mathrm{l}}(T_{\mathrm{S}} - T_{\mathrm{l}})]\left\{0.027\exp\left[\frac{0.08\sqrt{\mathrm{In}(\mathrm{we}/35+1)}}{B^{1.5}}\right] + 0.21k_{\mathrm{d}}B\exp\left[\frac{-90}{\mathrm{we}+1}\right]\right\} \tag{15}$$

where the Weber number,

$$\mathrm{we} = \frac{\rho_{\mathrm{l}} d {v_{\mathrm{n}}}^3}{\sigma} \tag{16}$$

the surface superheat parameter,

$$B = \frac{C_{\mathrm{v}}(T_{\mathrm{w}} - T)}{h_{\mathrm{fa}}} \tag{17}$$

and the dimensionless vapor parameter,

$$k_{\mathrm{d}} = \frac{\lambda_{\mathrm{v}}}{C_{\mathrm{v}}\mu_{\mathrm{v}}} \tag{18}$$

Then, the heat transfer quantity of all droplets contact with hot surface at per unit area and time can be expressed as:

$$q_{\mathrm{l}}'' = q_{\mathrm{d}} n$$

$$n = \frac{6Q_{\mathrm{l}}}{S\pi d^3} \tag{19}$$

where n is the number of droplets contact with hot surface per unit time, S is the coverage area of the spraying, Q_{l} is the volume flow rate of the cooling liquid, d is the average diameter of the droplets, ρ_{l} is the density of the cooling liquid, v_{n} is the normal velocity of the droplet, λ_{v} is the thermal conductivity of the vapor, μ_{v} is the viscosity of the vapor, and C_{v} is the specific heat of the vapor.

The heat transfer quantity of air convective is given by:

$$q_{\mathrm{a}}'' = 0.906\mathrm{Re}^{\frac{1}{2}}\mathrm{Pr}^{\frac{1}{3}}\frac{\lambda}{l}(T_{\mathrm{W}} - T_0) \tag{20}$$

Therefore, the heat transfer coefficient of the film boiling region can be expressed as:

$$h = \frac{q_{\mathrm{l}}'' + q_{\mathrm{a}}''}{T_{\mathrm{W}} - T_0} \tag{21}$$

3.4 The distribution of heat transfer coefficient on grinding surface

In this study, the air pressure is set to 0.6 Mpa; the liquid flow rate is 5 ml/min, and the air flow rate is 7.5 m^3/h. The hole diameter of the nozzle is 1.2 mm, and the nozzle is placed at a distance of about 30 mm from the grinding wheel–workpiece interface. The spraying diameter of the nozzle can cover the entire grinding surface of 8×4 mm (length × width). The grinding liquid is 5 vol.% water-based Al_2O_3 nanofluids. The heat transfer characteristic of the water-based Al_2O_3 nanofluids has been obviously improved in comparison with pure water since the Al_2O_3 nanoparticles have high thermal conductivity. The effective thermal conductivity of pure water can be improved by up to 23 % through the dispersion of 5 vol.% Al_2O_3 nanoparticles [20]. Therefore, the Al_2O_3 nanofluids were used for the cooling medium of MQL grinding.

According to the above mathematic model, the heat transfer coefficient in the non-boiling region (surface temperature T_{W}<105 °C) is 0.01 w/mm^2. It has increased eight to nine

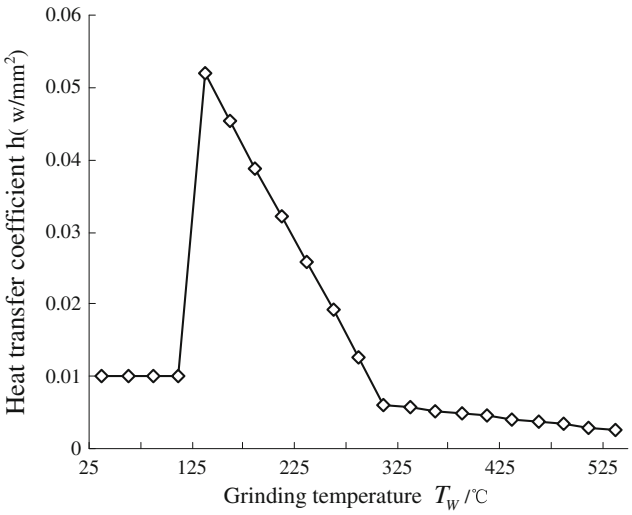

Fig. 2 The effect of grinding temperature on heat transfer coefficient

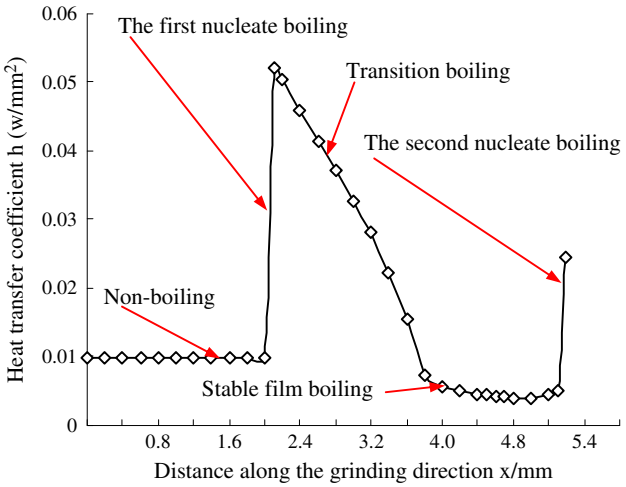

Fig. 3 The distribution of heat transfer coefficient in the grinding zone

times in comparison with bulk air convective heat transfer, which is agreed well with the research of Ye et al. [21]. In the nucleate boiling region (105 °C$<T_W<$125 °C), the heat transfer coefficient increases with the increase of the temperature, and it reaches the peak value of 0.052 w/mm^2 at the point of critical heat flux. However, in the transition boiling region (125 °C $< T_W <$300 °C), the heat transfer coefficient decreases with the rising temperature. In the stable film boiling region (300 °C $< T_W$), the curve relationship of heat transfer quantity and the grinding temperature is quite close to horizontal line based on Eqs. (15), (19) and (20). It has good agreement with the experimental result in the reference [11]. As the heat transfer coefficient is the ratio of heat transfer quantity to the temperature difference between the grinding temperature and the initial temperature of the grinding liquid, it shows a slightly decreasing trend in this region. The heat transfer coefficient is only 0.006 w/mm^2 when the temperature reaches to 300 °C. The relationship of heat transfer coefficient and the grinding temperature is shown in Fig. 2. The heat transfer coefficient can be approximately regarded as a constant in non-boiling region. In the nucleate boiling region, it immediately increases with the temperature rising, and it reaches a peak value at the point of critical heat flux. However, in the region of transition boiling and stable film boiling, it decreases with the temperature rising. The decline rate of transition boiling is quite large, and the stable film boiling tends to smooth. The distribution of heat transfer coefficient in the grinding zone is shown in Fig. 3. Nevertheless, the temperature distribution in the grinding zone is parabolic. In the ground surface, the heat transfer coefficient shows a linear distribution since the temperature is quite low. It presents a curve distribution in grinding zone where the temperature is quite high. It shows the second nucleate boiling heat transfer at the exit of grinding zone where the temperature is decreased sharply, as shown in Fig. 3.

4 Experiment

In order to verify the accuracy of the heat transfer coefficient, the temperature field for MQL grinding is analyzed by using the finite element method. In addition, the grinding temperature at the same grinding conditions as the simulation is measured by a single thermocouple. The experimental apparatus of the single thermocouple is shown in Fig. 4.

The grinding experiments were conducted on the ultra-precision surface grinder. A ceramic bond aluminum oxide grinding wheel (WA46) was used, and the diameter of the grinding wheel is 200 mm. The workpiece and clamping device were fixed on the three-dimensional piezoelectric crystal dynamometer, as shown in Fig. 1. The material of the workpiece is AISI52100. The thermal conductivity coefficient and the specific heat capacity of the workpiece are 41 W/m K and 371 J/Kg K, respectively. The speed of the grinding wheel is 31.4 m/s. The speed of the workpiece is 0.1 m/s. The moving direction of the workpiece is adverse to the rotating tangent direction of the grinding wheel. The cutting depth is 25 μm. The Al_2O_3 nanofluids are used for cooling medium. The grinding conditions are summarized in Table 1.

It is well known that the grinding temperature of the workpiece is directly affected by the wheel–workpiece real contact length and the heat flux which entered into the workpiece [22]. For the calculation of the wheel–workpiece

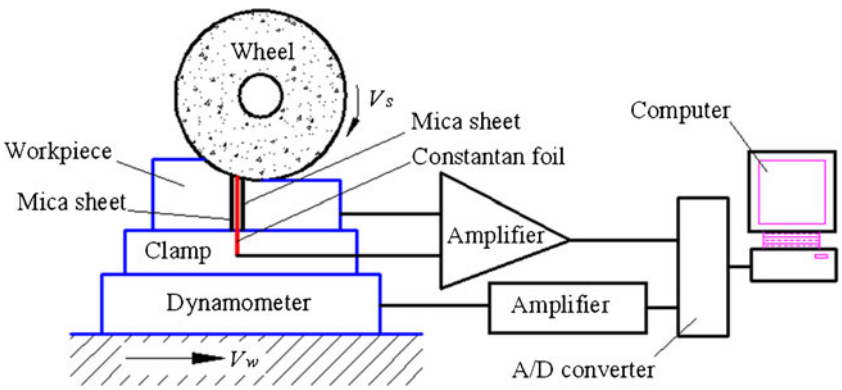

Fig. 4 The experimental apparatus of the single thermocouple

Table 1 Grinding conditions

Grinding wheel	WA46
Wheel diameter (mm)	d=200
Wheel speed (m/s)	v_s=31.4
Work material	AISI52100
Table speed (m/s)	v_w=0.1
Cutting depth (μm)	a_p=25
Grinding state	Up grinding
Grinding fluid	Al_2O_3 nanofluids

real contact length and the heat flux which entered into the workpiece, see the previous research by the authors [23]. In the simulation, the heat load is applied on the related grinding surface at different time steps. The simulated result of grinding surface temperature is shown in Fig. 5. The grinding temperature measured by a single thermocouple is shown in Fig. 6. An example temperature field is shown in Fig. 7. As shown in Fig. 6, the workpiece experiences an elevated background temperature at the surface due to the distributed action of all the abrasive grains on the wheel operating in the grinding zone. Localized temperatures at the abrasive–wear flat interface, which are illustrated by the spikes, elevated above the background temperature.

It can be seen from Figs. 5 and 6 that the simulative temperature is really close to the experimental temperature. The peak temperatures of simulating and measuring are 447.6 and 460.4 °C, respectively. It is obvious that the peak temperature of the measuring is slightly higher than that of the simulating. This is probably attributed to the heat inertia of the thermocouple. The node must be heated for a period of time before it reaches the temperature value of workpiece surface. In addition, the instrument is a little unresponsive for the signal-processing so that it could not keep up with the changing of the actual heat signal. It can also be seen from Figs. 5 and 6 that the simulative temperature falls faster than the experimental temperature on the ground surface. The probable reason which results in this phenomenon is that the

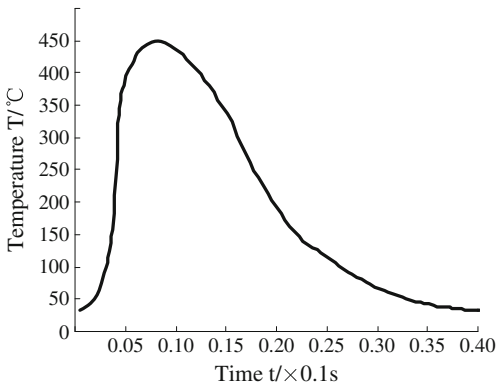

Fig. 5 The simulative temperature distribution in the grinding zone

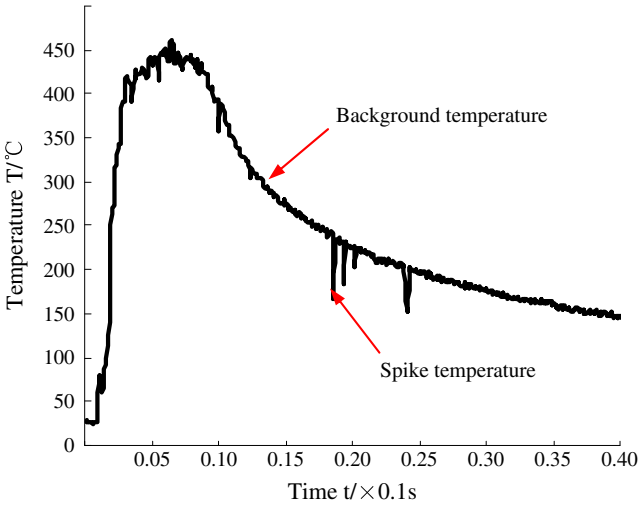

Fig. 6 The experimental temperature distribution in the grinding zone

heat resistance of the mica sheet in the single pole thermocouple is higher than steel, which slowers the diffusion speed of the heat into the workpiece. The good agreement between the simulative result and experimental measuring value shows that the theory of surface heat transfer coefficient during MQL grinding is creditable.

5 Conclusions

The heat transfer coefficient on workpiece surface during MQL grinding is analyzed, and the simulation of grinding surface temperature based on the theory of surface heat transfer coefficient during MQL grinding is carried out. The simulative result and the experimental measurement

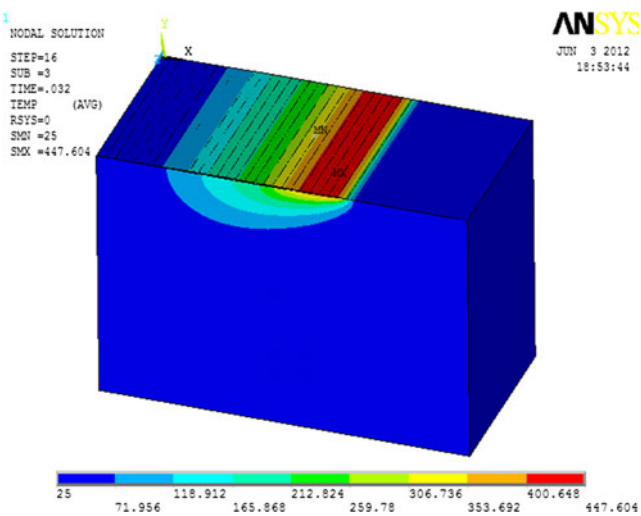

Fig. 7 The temperature field at the 16th load step

result are compared. The main conclusions are summarized as follows:

(1) The grinding zone is divided into four different regions according to the heat transfer mechanism of droplet at different surface temperatures, namely non-boiling heat transfer region, nucleate boiling heat transfer region, transitional boiling heat transfer region and stable film boiling heat transfer region. Furthermore, the related mathematical models of heat transfer in the grinding zone are established.

(2) The heat transfer coefficient can be approximately regarded as a constant in the non-boiling region. In the nucleate boiling region, it immediately increases with the temperature rising, and it reaches the peak value at the point of critical heat flux. However, in the regions of transition boiling and stable film boiling, the heat transfer coefficient decreases with the temperature rising. The decline rate in the transition boiling region is quite large, and the stable film boiling tends to smooth.

(3) The surface grinding experiment is carried out; a good agreement is found between the simulative result and the experimental measuring result of the surface temperature during MQL grinding, which shows that the theory of surface heat transfer coefficient during MQL grinding is creditable.

(4) We can predict the quantity of heat transfer at any point on workpiece surface during MQL grinding by using the heat transfer model proposed in this study, which provides the theory foundation for grinding surface temperature field.

Acknowledgments This project was sponsored by the National Natural Science Foundation of China (grant No. 51005024), the Hunan Provincial Natural Science Foundation of China (grant No. 10JJ3056) and the Scientific Research Fund of Hunan Provincial Education Department (grant No. 10C0364).

References

1. Mao C, Zhou ZX, Zhang J, Huang XM, Gu DY (2011) An experimental investigation of affected layers formed in grinding of AISI 52100 steel. Int J Adv Manuf Technol 54(5):515–523
2. Tasdelen B, Thordenberg H, Olofsson D (2008) An experimental investigation on contact length during minimum quantity lubrication (MQL) machining. J Mater Proc Technol 203:221–231
3. Nam JS, Lee PH, Lee SW (2011) Experimental characterization of micro-drilling process using nanofluid minimum quantity lubrication. Int J Mach Tool Manuf 51:649–652
4. Asif I, He N, Iqbal K, Li L, Naeem UD (2008) Modeling the effects of cutting parameters in MQL-employed finish hard-milling process using D-optimal method. J Mater Proc Technol 199:379–390
5. Dhar DR, Kamruzzaman M, Ahmed M (2006) Effect of minimum quantity lubrication (MQL) on tool wear and surface roughness in turning AISI-4340 steel. J Mater Proc Technol 172:299–304
6. Tawakoli T, Hadad MJ, Sadeghi MH, Daneshi A, Stöckert S, Rasifard A (2009) An experimental investigation of the effects of workpiece and grinding parameters on minimum quantity lubrication—MQL grinding. Int J Mach Tool Manuf 49:924–932
7. Mei GH, Meng HJ, Wu RY, Ci Y, Xie Z (2004) Analysis of spray cooling heat transfer coefficient on high temperature surface. Energy Metalll Ind 23(6):18–22
8. Deb S, Yao SC (1989) Analysis on film boiling heat transfer of impacting spray. Heat Mass Transf 32:2099–2112
9. Shen B, Shih AJ, Tung SC (2008) Application of nanofluids in minimum quantity lubrication grinding. Tribol Trans 51:730–737
10. Feng BF, Cai GQ, Pan XJ, Gai QW (2002) Coolant supplying methods in high-speed grinding. Mach Tool Hydraul 2:173–175
11. Zhang CY (2008) Study on the mechanism of MQL cutting and its application fundament. Jiangsu University, Zhenjiang
12. Wang ZX, Yu CY, Zhou CJ (2003) Spray drying. Chemical Industry, Beijing
13. Liu L (1984) Analysis of heat transfer during spray cooling. Iron Steel 19:63–70
14. Zhang JZ, Chang HP (2009) Heat transfer. Science, Beijing
15. Liu ZH (1997) Experimental study on the boiling critical heat flux of mist cooling. J Shanghai Jiaotong Univ 31:61–65
16. Cabrera E (2003) Heat flux correlation for spray cooling in the nucleate boiling regime. Exp Heat Transf 16:19–44
17. Chen WK, Luo X, Zhang CM, Lu MH, Ma HG (2007) Experimental study on spray impinging evaporation under small temperature differences. J Eng Thermophys 28:277–279
18. Visaria M, Mudawar I (2008) Effects of high subcooling on two-phase spray cooling and critical heat flux. Int J Heat Mass Transfer 51:2398–2410
19. Wang YQ (2010) Research on the characters of non-boiling heat transfer for spray cooling. University of Science and Technology of China, Anhui
20. Xie H, Wang J, Xi T et al (2002) Dependence of the thermal conductivity of nanoparticle–fluid mixture on the base fluid. J Mater Sci Lett 21:1469–1471
21. Ye L, Tong ZM, Zhu RH, Li N (2006) Characters of heat transfer processes under spray conditions. Chem Ind Eng Prog 55:248–252
22. Zhao HH, Cai GQ, Li CH, Jin T (2004) Study on grinding temperature and surface burn out in high efficiency deep grinding. China Mech Eng 22:2048
23. Mao C, Zhou ZX, Zhou DW, Yang J (2009) Research on three dimensional finite element simulation of the temperature field in surface grinding. China Mech Eng 20:589–595